

Scanning tunneling spectroscopy on crossed carbon nanotubes

J. W. Janssen, S. G. Lemay, L. P. Kouwenhoven, and C. Dekker

Applied Physics and DIMES, Delft University of Technology, Lorentzweg 1, 2628 CJ Delft, The Netherlands

(Received 3 October 2001; published 8 March 2002)

Crossing nanotubes were investigated using scanning tunneling microscopy (STM) and spectroscopy. From the analysis of the measured mechanical deformation of the nanotubes, the contact force between the nanotubes is estimated to be 1 nN. Spectroscopy measurements showed two effects on the electronic structure: (i) band bending, which we attribute to a position-dependent interaction with the substrate, and (ii) the formation of localized states, as signalled by additional peaks in the density of states at the crossing point. The existence of localized states at the junction represents a much stronger perturbation of the electronic structure than has generally been assumed. The relevance of these STM results for the interpretation of transport measurements is discussed.

DOI: 10.1103/PhysRevB.65.115423

PACS number(s): 73.22.-f, 85.35.Kt, 07.79.Cz, 62.25.+g

I. INTRODUCTION

Since carbon nanotube molecules have been electrically contacted^{1,2} a variety of single nanotube electronic devices has been fabricated. These include devices based on an individual single wall carbon nanotube (SWNT) such as field-effect transistors,^{3,4} single-electron transistors,⁵ and diodes.⁶ More complex arrangements involving more than one SWNT have also been fabricated recently using atomic force microscope (AFM) manipulation,⁷ and crossed nanotube junctions have been contacted to produce multiterminal nanotube devices.⁸

Such nanotube junctions are the subject of this paper. From transport measurements, Fuhrer *et al.* proposed that nanotube junctions can exhibit two different types of behavior.⁸ The behavior of a crossing between two metallic or two semiconducting tubes was interpreted as a conventional tunnel contact at the junction. The behavior of a crossing between a metallic and a semiconducting SWNT was instead interpreted as a Schottky barrier combined with a tunnel contact. Both these and other measurements⁷ could be explained by assuming that the bulk electronic properties of each nanotube were not severely affected by the presence of the junction. The validity of this assumption is difficult to ascertain by transport measurements, however, since the latter provide only indirect information about the local electronic structure near the junction.

Scanning tunneling microscopy (STM) and spectroscopy (STS) are ideally suitable to tackle this problem. On carbon nanotubes, STM and STS have confirmed the relation between the atomic structure and the electronic properties.^{9,10} More recently, the effect of strong bends (buckles)¹¹ and kinklike topological defects¹² have been studied. Here we use STM to study nanotube crossings. We estimate the force between the nanotubes and their binding energy to a supporting gold substrate. More importantly, our STS studies show that the local electronic structure can be severely distorted due to the crossing. We observe two effects on the electronic structure: (i) band bending, which we attribute to a position-dependent interaction with the substrate, and (ii) localized states, as signalled by additional peaks in the density of states at the crossing point. The existence of localized states at the junction represents a much stronger perturbation of the

electronic structure than has generally been assumed, and is highly relevant for the interpretation of transport measurements.

The outline of this paper is as follows. We first present the topographic images of crossed carbon nanotubes (Sec. II). Using a simple continuum model we estimate the force between the tubes from these topographic images (Sec. III), and compare this with results from theoretical calculations. The results of STS measurements are then presented (Sec. IV) and their implications are discussed (Sec. V).

II. TOPOGRAPHY RESULTS

Single wall carbon nanotubes (SWNT's) were produced using laser evaporation by the group of R. E. Smalley at Rice University, Houston. A small amount of the raw material was ultrasonically dispersed in dichloroethane. A few droplets were deposited on gold (111) facets, which were formed by flame annealing a small (15 mm³) piece of 99.99% pure gold. This procedure results in (mainly individual) carbon nanotubes on an atomically flat surface. Such a sample was cooled down in a home-built 4-K STM,¹³ and scanned with 90% Pt-10% Ir tips cut under ambient conditions. Nanotubes crossing other nanotubes were regularly found.

Eight of these crossings have been studied in detail. Three typical examples are shown in Fig. 1. All three topographs were obtained using a sample bias voltage of -1 V and a feedback current of 20 pA. The two tubes in Fig. 1(a) cross at a 26° angle, while those in Figs. 1(b) and (c) cross at 90° angles. The diameter of these SWNT's is ~ 1.5 nm, as determined from height measurements. The nanotubes can appear up to 15 nm in width in the images due to tip convolution.

Height profiles along the longitudinal axis of the uppermost tube are shown below each image in Fig. 1. These plots show that a tube crossing another tube does not closely follow the height profile of the obstacle. The deformations associated with the crossings instead occur over lengths of 40 nm in Fig. 1(a), 60 nm in Fig. 1(b), and 35 nm in Fig. 1(c). The height profiles are thus smooth on a length scale much longer than the diameter of the underlying SWNT and the size of the STM tip. This reflects the intrinsic stiffness of the SWNT's.

The top tube in Fig. 1(a) [(b), (c)] has a diameter of 1.6

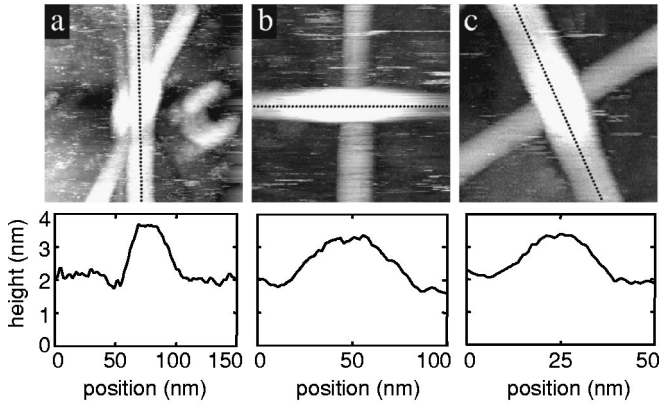


FIG. 1. Topographic images of three crossings between pairs of individual SWNT's. These images were obtained using a feedback current of 20 pA at a sample voltage of -1 V. The height profile along the dotted line in each image is plotted below the image. The gold substrate is taken as reference height.

(1.5, 1.7) nm. Here 0.3 nm was subtracted from the topographic height to account for the van der Waals distance.¹⁴ These values are in good agreement with values for the diameter deduced from spectroscopy measurements.¹⁵ In Fig. 1(a) [(b), (c)] the underlying tube is 1.7 (1.5, 1.4) nm in diameter. The total height of the crossing is 3.2 (2.9, 3.0) nm and is thus lower by 20–23% than the sum of the diameters of both tubes plus the van der Waals distances. This indicates that a certain amount of mechanical deformation (“squashing”) of the nanotubes exists at the crossings. From the smoothness of the height profiles at the junction, we can, however, exclude the presence of local buckles at the crossing.

III. DETERMINATION OF THE CONTACT FORCE

In this section we discuss how the contact force between the nanotubes at the crossing can be calculated from the measured height profiles. The magnitude of this force provides a quantitative measure of the strength of the interaction between the nanotubes and of the deformation of the nanotubes at the crossing. It also allows for comparison with theoretical calculations which additionally assess the impact of the crossing on the tubes' electronic interaction. We calculate the contact force using a simple continuum model, similar to models used in discussions of the mechanical properties of carbon nanotubes.^{16,17}

A nanotube on a gold substrate feels an attractive force from the substrate due to the van der Waals interaction. When a nanotube crosses another nanotube (or other obstacle) the upper nanotube deforms elastically by slightly bending over the lower nanotube. This induces strain in the upper nanotube, resulting in a normal contact force between the nanotubes. The situation is similar to the model of a centrally loaded cylinder with fixed ends.¹⁸

The force exerted at the area of contact is given in this case by $F = 192EIh/l^3$, where E is the Young's modulus, I the second moment of area, h the central deflection of the upper tube, and l the length over which the tube is bent or deformed. Values for both h and l can be obtained from the

height profiles in Fig. 1. The Young's modulus of an individual SWNT has previously been estimated to have the value $E = 1.3 \pm 0.4$ TPa from deflection measurements on multiwall nanotubes (MWNT's) and ropes of SWNT's.¹⁶ A SWNT can be approximated as a hollow cylinder with a second moment of area $I = (\pi/4)(r_{outer}^4 - r_{inner}^4)$. Here r_{outer} and r_{inner} are the outer and inner radius, respectively. They can be estimated from the measured diameter using 0.3 nm as the wall thickness for an individual tube.¹⁴ Typical values for our junctions are $r_{outer} = 0.9 \pm 0.1$ nm and $r_{inner} = 0.6 \pm 0.1$ nm, $h = 1.5 \pm 0.1$ nm and $l = 50 \pm 5$ nm. This yields a force ranging from 0.6 to 1.2 nN for different junctions, with a typical uncertainty of 0.3 nN for each case. For comparison, the force exerted by the STM tip is estimated not to exceed 0.05 nN for the scan parameters used.¹⁹ As this force is significantly smaller than the intertube force of ~ 1 nN, we neglect effects from tip forces.

The estimated contact force of 1 nN can be compared to theoretical calculations. In Ref. 17 it was argued, based on continuum and molecular mechanics simulations, that two crossing (10,10) tubes on a graphite surface exhibit a contact force of 5 nN. This is of the same order of magnitude as our experimental results, which were obtained for tubes with diameters similar to a (10,10) tube. In the simulations, the force pressing the two tubes together reduces the total height of the crossing by 20%. This fits very well with our observation of 20–23% height reduction.

The intertube conductance at crossings with a geometry very similar to that studied here was measured by Fuhrer *et al.*⁸ to be as high as $0.2 e^2/h$. This corresponds to 10% of the value for perfect transmission, $2e^2/h$. The dependence of the conductance between two crossing (5, 5) nanotubes on the contact force was investigated in calculations by Yoon *et al.*,²⁰ and a strong dependence on the contact force was found. For a contact force of 1–2 nN (corresponding to our experimentally determined force), a low intertube conductance ($< 0.05e^2/h$) was predicted. The experimental results by Fuhrer *et al.* were best explained by contact forces of 10–15 nN. At such high contact forces it was calculated that there is a significant mechanical deformation of the nanotubes resulting in an enhancement of the wave-function overlap between the nanotubes. It was further concluded that the intratube conductance is, however, only weakly affected by the presence of the crossing. We will return to these calculations in Sec. V.

Analysis of the height profile can also be used to estimate the binding energy of nanotubes on gold using the method of Hertel *et al.*²¹ Briefly, this involves balancing the cost of elastically bending the nanotube and the gain in binding energy to the substrate. The binding energy is obtained by integrating $\frac{1}{8}E\pi(r_{outer}^4 - r_{inner}^4)\int \rho(x)^{-2}dx$ along the longitudinal axis of the tube. Here $\rho(x)$ is the local radius of curvature. Our profiles are well fitted by a circle with a typical radius of ~ 100 nm. We then obtain a binding energy of 0.8 ± 0.2 eV/Å. The results for different crossings range from 0.5 to 1.2 eV/Å. A similar binding energy of 0.8 ± 0.3 eV/Å was obtained by Hertel *et al.* for MWNT's on hydrogen-passivated silicon.²¹

IV. SPECTROSCOPY RESULTS

We now turn to the effect of a crossing on the electronic structure of the SWNT's. We have performed STS measurements on the upper nanotube as a function of position for a number of crossings. In STS, the STM tip is held at a fixed distance from the sample and the differential tunnel conductance dI/dV is measured as a function of tip-sample bias V . It can be shown that $dI/dV(V)$ is approximately proportional to the density of states (DOS) at energy eV .²² Such measurements were repeated on a series of equally spaced positions along the longitudinal axis of the tube with sub-Ångstrom resolution. We find that a crossing can have two different effects on the local electronic structure in a carbon nanotube, viz., band bending (i.e., spatially dependent energy bands) and the formation of localized states.

For reference, we first discuss spectroscopy results on straight nanotubes lying on a gold or platinum substrate. Figure 2(a) shows the DOS as a function of position for a semiconducting nanotube on atomically flat gold. dI/dV is plotted in grayscale as a function of position on the tube (x axis) and sample voltage (y axis). For clarity a single $dI/dV(V)$ curve is also shown on the right. The white area in the grayscale plot corresponds to the semiconducting gap and is bordered by two van Hove singularities (VHS's). A VHS marks the onset of a one-dimensional band in the carbon nanotube band structure. In this figure we observe the VHS for the conduction band at $+1.0$ V and for the valence band at -0.1 V. In the valence band, the second VHS is visible at -0.6 eV. The energies of the VHS are normally assumed to be independent of position. Figure 2(a) however, exhibits small (~ 0.05 eV) variations in these energies, even in this simple case of a nanotube on an atomically flat surface. A more dramatic effect is evident in Fig. 2(b), which shows the case of a tube lying on a platinum substrate. This surface is not atomically flat but instead consists of grains with a typical lateral size of 20 nm. The corrugation between the peaks and valleys of the grains is 1.5–2 nm. The height profile (plotted below the STS plot) shows that the corrugation on the nanotube is, however, only 0.5 nm. The nanotube thus does not follow the contour of the grains, but instead hangs in between grains at both $x \approx 13$ and $x \approx 32$ nm due to its stiffness. In the DOS(x) plot, a shift of the semiconducting gap towards negative energies is observed at these positions. We interpret this shift as a change in the amount of charge transfer between the nanotube and the substrate (“doping”) due to variations in the strength of interaction with the substrate. Such band bending is also exploited in nanotube field-effect transistors.³

Figure 2(c) shows STS measurements for a semiconducting nanotube crossing another semiconducting nanotube [see Fig. 1(a)]. At the onset of the valence band a dotted line is plotted as a guide to the eye. The second VHS in the valence band is also visible. Following the position in energy of the VHS along the length of the tube, we observe energy fluctuations of about 0.25 eV. Similar fluctuations are also observed in the energy of the first VHS of the conduction band. The fluctuations in both valence and conduction band are strongly correlated, indicating local band bending. Since

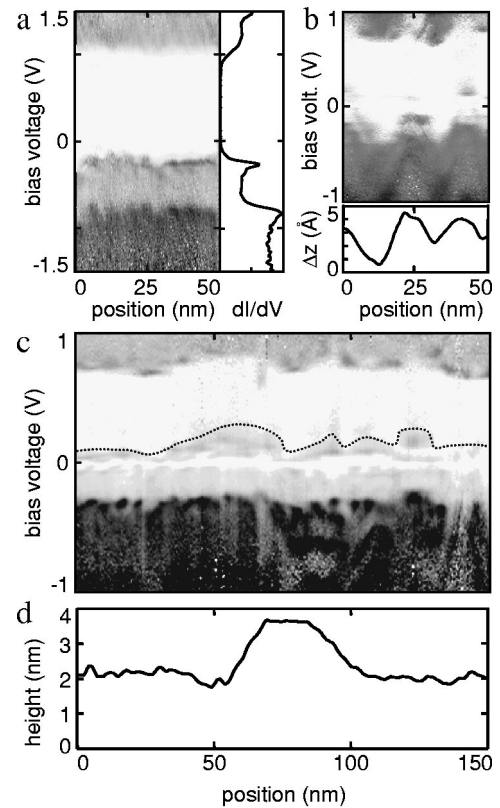


FIG. 2. (a) The differential conductance dI/dV for a semiconducting tube lying on an atomically flat gold substrate shown as a function of sample voltage (y axis) and position along the nanotube (x axis). The grayscale indicates the magnitude of dI/dV : white corresponds to 0 nA/V, black to 0.2 nA/V. A single $dI/dV(V)$ curve is also plotted on the right for reference. (b) Grayscale plot of $dI/dV(V)$ as a function of position for a semiconducting SWNT lying on a granular platinum substrate. Black corresponds to 0.6 nA/V. The height profile along the nanotube is plotted below. (c) Grayscale plot of $dI/dV(V)$ as a function of position for a semiconducting SWNT crossing another semiconducting SWNT [Fig. 1(a)]. Black corresponds to 0.2 nA/V. The onset of the first van Hove singularity at the valence band edge is marked by a dotted line. Fluctuations of the energy of the valence and conduction band edges are highly correlated. (d) Height versus position; the crossing is located at $x \approx 80$ nm.

such large fluctuations are not normally observed for tubes lying flat on an Au(111) surface, we attribute them to the presence of the crossing. Accounting quantitatively for these fluctuations is difficult because several parameters are poorly known (e.g., the amount of charge transfer at the nanotube-nanotube junction), and this will not be discussed further here.

In addition to band bending, crossings can exhibit more severe perturbations of the electronic structure, namely the formation of additional states. Figures 3(a)–(c) show STS data taken along a metallic tube crossing over a semiconducting tube [Fig. 1(b)]. The central region in energy, with a width of ~ 1.8 eV, is bordered by two van Hove singularities at about -0.8 and 1.0 eV, as shown in Fig. 3(a).²³

The height profile over the junction is also plotted in Fig. 3(d). At the top of the crossing, near $x = 50$ nm, two peaks in

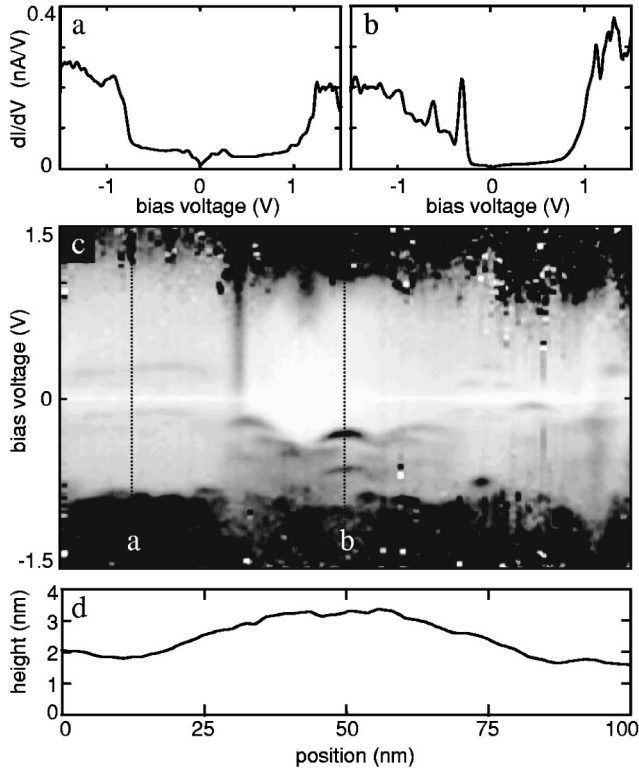


FIG. 3. Differential conductance for a metallic SWNT crossing a semiconducting SWNT [Fig. 1(b)]. (a) Differential conductance dI/dV versus sample bias V far from the crossing. The DOS is finite around near the Fermi level, and van Hove singularities are observed at -0.8 and ~ 1.0 eV. (b) $dI/dV(V)$ at the position of the crossing. Two additional peaks are visible at -0.3 and -0.6 eV, whereas the DOS in the pseudogap is suppressed between -0.2 and $+0.3$ eV. (c) Grayscale plot of the differential conductance as a function of sample bias voltage (y axis) and position along the metallic tube (x axis). White corresponds to 0 nA/V, black to 0.2 nA/V. The dotted lines indicate the positions of the curves shown in (a) and (b). (d) Height versus position; the crossing occurs at $x \approx 50$ nm.

the DOS appear, as emphasized in Fig. 3(b). The black areas indicate an enhanced DOS at -0.3 eV and -0.6 eV. These states are highly localized near the crossing. At the same position we observe a reduction in the DOS at energies between -0.2 and 0.3 eV, which appears as a white region in Fig. 3(c). These features are qualitatively consistent with Coulomb blockade for tunneling into a small island. An estimate for the size of such an island can be obtained from the energy spacing $\Delta E = 0.3$ eV between the two localized peaks. Using $L = \hbar v_f / 2\Delta E$, where \hbar is Planck's constant and $v_f = 8.2 \times 10^7$ cm/s,²⁴ we obtain $L = 6$ nm. This agrees well with the observed extension of about 8 nm. Tip convolution does not have a big effect since the height change on top is small in the length direction of the nanotube.

Localized states can arise from severe topological distortions like buckles,^{25,26} in which atomic bonds are rearranged. As discussed in Sec. II, however, such a distortion is unlikely to be present here. This strongly suggests that the interaction between the tubes at the crossing is responsible for the features observed.

V. DISCUSSION AND CONCLUSIONS

The contact force that we determine experimentally would, according to calculations,²⁰ result in a weak electrical contact between the nanotubes. These calculations suggested that backscattering due to the crossing is very weak and that the intratube conductance is only slightly reduced. We instead observe a severe distortion of the electronic structure even in the case of small forces and expect this to have a significant impact on backscattering. Direct comparison is, however, not possible since published simulations only provide information on the conductance, whereas our experiment only measures the local density of states.

The layout of our crossings is very similar to that used in transport measurements,^{7,8} but the underlying substrates [SiO_2 for transport measurements and Au(111) for STM measurements] differ. Nonetheless, the binding energy between nanotube and substrate²¹ and the height profile at the crossing⁷ are comparable in the two cases. We therefore expect changes in the electronic structure induced by the crossing to also be comparable. The interpretation of the transport measurements has so far been based on tunneling between nanotubes whose bulk electronic properties are not affected by the crossing. We have shown here that the local electronic structure can instead be severely distorted, that is, that the bulk electronic properties can be strongly affected. This is further supported by recent electrostatic force microscopy (EFM) measurements which found that a large intratube resistance is present at the crossing.²⁷

It has been suggested that carbon nanotube crossings provide an excellent opportunity to probe the interaction between Luttinger liquids, and some experiments have already been interpreted in this context.^{7,28} Calculations so far have, however, neglected scattering due to the presence of the crossing.²⁹ The effect of scattering is expected to be large since, for example, an impurity is predicted to lead to vanishing conductance in a Luttinger liquid at $T=0$. Our observation of a severe distortion of the electronic structure at the crossing implies that the approximation of negligible scattering probably does not hold under current experimental conditions. Additional experiments which minimize the amount of mechanical strain at the crossing, or corrections to the theory to include the role of this strain, will be required to resolve this matter.

In summary, we have presented STM and STS results on SWNT junctions. From analysis of topography measurements, we estimated the contact force between crossing nanotubes to be at most 1 nN. Spectroscopy measurements on crossed tubes show clear modifications of the band structure due to the crossing. Two types of effects were observed: band bending which we attribute to nonuniform doping by the substrate, and localized states due to interactions between the nanotubes at the crossing.

ACKNOWLEDGMENTS

The nanotube material was kindly supplied by R. E. Smalley and co-workers at Rice University. This research was financially supported by the Dutch Foundation for Fundamental Research on Matter (FOM) and the European Community SATURN Project. S.G.L. acknowledges additional support from NSERC of Canada.

- ¹S.J. Tans, M.H. Devoret, H. Dai, A. Thess, R.E. Smalley, L.J. Geerligs, and C. Dekker, *Nature (London)* **386**, 474 (1997).
- ²M. Bockrath, D.H. Cobden, P.L. McEuen, N.G. Chopra, A. Zettl, A. Thess, and R.E. Smalley, *Science* **275**, 1922 (1997).
- ³S.J. Tans, A.R.M. Verschueren, and C. Dekker, *Nature (London)* **393**, 49 (1998).
- ⁴R. Martel, T. Schmidt, H.R. Shea, T. Hertel, and Ph. Avouris, *Appl. Phys. Lett.* **73**, 2447 (1998).
- ⁵H.W.Ch. Postma, T. Teepen, Z. Yao, M. Grifoni, and C. Dekker, *Science* **293**, 76 (2001).
- ⁶Z. Yao, H.W.Ch. Postma, L. Balents, and C. Dekker, *Nature (London)* **402**, 273 (1999).
- ⁷H.W.Ch. Postma, M. de Jonge, Z. Yao, and C. Dekker, *Phys. Rev. B* **62**, 10 653 (2000).
- ⁸M.S. Fuhrer, J. Nygard, L. Shih, M. Forero, Young-Gui Yoon, M.S.C. Mazzoni, Hyoung Joon Choi, Jisoon Ihm, Steven G. Louie, A. Zettl, and Paul L. McEuen, *Science* **288**, 494 (2000).
- ⁹J.W.G. Wildöer, L.C. Venema, A. Rinzler, R.E. Smalley, and C. Dekker, *Nature (London)* **391**, 59 (1998).
- ¹⁰T. Odom, J.-L. Huang, P. Kim, and C. Lieber, *Nature (London)* **391**, 62 (1998).
- ¹¹J.W. Janssen, S.G. Lemay, M. van den Hout, M. Mooij, L.P. Kouwenhoven, and C. Dekker, *Kirchberg 2001 Conference Proceedings*, edited by H. Kuzmany, J. Fink, M. Mehring, and S. Roth, AIP Conf. Proc. No. 591 (AIP, Melville, NY, 2001), pp. 293–297.
- ¹²M. Ouyang, J.-L. Huang, C.L. Cheung, and C.M. Lieber, *Science* **291**, 97 (2001).
- ¹³J.W.G. Wildöer, A.J.A. van Roy, H. van Kempen, and C.J.P.M. Harmans, *Rev. Sci. Instrum.* **65**, 2849 (1994).
- ¹⁴J. Israelachvili, *Intermolecular & Surface Forces* (Academic, London, 1994).
- ¹⁵L.C. Venema, J.W. Janssen, M.R. Buitelaar, J.W.G. Wildöer, S.G. Lemay, L.P. Kouwenhoven, and C. Dekker, *Phys. Rev. B* **62**, 5238 (2000). We use 2.6 eV as the value for the overlap integral γ_0 ; see Ref. 24.
- ¹⁶For a review, see A. Krishnan, E. Dujardin, T.W. Ebbesen, P.N. Yianilos, and M.M.J. Treacy, *Phys. Rev. B* **58**, 14 013 (1998), and references therein.
- ¹⁷T. Hertel, R.E. Walkup, and Ph. Avouris, *Phys. Rev. B* **58**, 13 870 (1998).
- ¹⁸A.H. Cottrell, *The Mechanical Properties of Matter* (John Wiley & Sons, New York, 1964).
- ¹⁹R. Wiesendanger, *Scanning Probe Microscopy and Spectroscopy* (Cambridge University Press, Cambridge, England, 1994).
- ²⁰Y.G. Yoon, M.S.C. Mazzoni, H.J. Choi, J. Ihm, and S.G. Louie, *Phys. Rev. Lett.* **86**, 688 (2001).
- ²¹T. Hertel, R. Martel, and Ph. Avouris, *J. Phys. Chem. B* **102**, 910 (1998).
- ²²J. Tersoff and D.R. Hamann, *Phys. Rev. B* **31**, 805 (1985).
- ²³A small suppression of the DOS can also be seen near zero bias with an energy width of ~ 50 meV at all positions. This feature is present in most of our STS measurements on metallic SWNT's (Ref. 15) and will be discussed separately.
- ²⁴S.G. Lemay, J.W. Janssen, M. van den Hout, M. Mooij, M.J. Bronikowski, P.A. Willis, R.E. Smalley, L.P. Kouwenhoven, and C. Dekker, *Nature (London)* **412**, 617 (2001).
- ²⁵S. Iijima, C. Brabec, A. Maiti, and J. Bernholc, *J. Chem. Phys.* **104**, 2089 (1996).
- ²⁶A. Rochefort, Ph. Avouris, F. Lesage, and D.R. Salahub, *Phys. Rev. B* **60**, 13 824 (1999).
- ²⁷A. Bachtold (private communications); the measurement method is described in A. Bachtold, M.S. Fuhrer, S. Plyasunov, M. Forero, E.H. Anderson, A. Zettl, and Paul L. McEuen, *Phys. Rev. Lett.* **84**, 6082 (2000).
- ²⁸J. Kim, K. Kang, J. Lee, K. Yoo, J. Kim, J. Park, H. So, and J. Kim, cond-mat/0005083 (unpublished).
- ²⁹A. Komnik and R. Egger, *Phys. Rev. Lett.* **80**, 2881 (1998).